All-solid antiresonant fiber design for high-efficiency three-level lasing in ytterbium-doped fiber lasers

Goel, Charu; Yoo, Seongwoo

2022

Goel, C. & Yoo, S. (2022). All-solid antiresonant fiber design for high-efficiency three-level lasing in ytterbium-doped fiber lasers. Optics Letters, 47(5), 1045-1048. https://dx.doi.org/10.1364/OL.453781

https://hdl.handle.net/10356/156835

https://doi.org/10.1364/OL.453781

All-solid antiresonant fiber design for high-efficiency three-level lasing in ytterbium-doped fiber lasers

CHARU GOEL[1] AND SEONGWOO YOO[1,*]

[1] *The Photonics Institute, School of Electrical and Electronics Engineering, Nanyang Technological University, 50 Nanyang Avenue, Singapore 639798*

**Corresponding author: seon.yoo@ntu.edu.sg*

Received XX Month XXXX; revised XX Month, XXXX; accepted XX Month XXXX; posted XX Month XXXX (Doc. ID XXXXX); published XX Month XXXX

We propose and investigate an all-solid ytterbium-doped antiresonant fiber (YbARF) design to inherently suppress four-level lasing with >20 dB/m of selective loss and achieve high-efficiency three-level lasing, while maintaining near-diffraction limited operation with ultra-large mode area of ~3630 μm². The YbARF is designed so that the high-gain wavelengths corresponding to four-level lasing lie in the resonance band characterized by high confinement loss. This enables three-level lasing with high efficiency in a short (0.8 m long) YbARF, making it a potential candidate for high peak power, ultrafast lasers at 976 nm. We discuss fiber design considerations and detailed simulation results for three-level lasing performance in the YbARF, promising >85% lasing efficiency in single-pass pump configuration. The design concepts can be easily extended to suppress high-gain wavelengths in other rare earth doped fiber amplifiers or lasers like thulium, erbium, and neodymium.

1. INTRODUCTION

Large mode area (LMA) fibers are important for mitigating nonlinearities in high-power laser applications, and it is equally desirable to have single mode operation in these fibers to maintain good beam quality and suppress transverse mode instabilities. Several effectively single-mode ytterbium (Yb)-doped LMA fiber designs have been reported in the past and high-efficiency quasi four-level lasing at around 1030 nm has been demonstrated [1-4]. Yb ions in silica host have another emission peak at around 976 nm, corresponding to a three-level transition and high-power laser sources in that wavelength range have significant research interest because of their application as core-pumping sources for Erbium (Er^{3+}) and Yb co-doped fiber lasers and amplifiers. Moreover, 976 nm laser sources may be frequency-converted to 488 nm blue radiation to replace bulky Argon-ion lasers for biomedical applications and underwater exploration of marine resources [5].

High-efficiency three-level lasing in Yb-doped fibers is challenging because the absorption and emission cross-sections of Yb are nearly equal at around 976 nm, necessitating >50% population inversion throughout the active fiber. On the other hand, the competing four-level transition at ~1030 nm has higher ratio of emission to absorption cross-section, implying that parasitic lasing and amplified spontaneous emission (ASE) at that wavelength can develop even at low population inversion. It is therefore imperative to suppress the high gain four-level lasing wavelengths to enable lasing at around 976 nm. Large core-to-cladding area ratio (CCAR) in cladding-pumped cavities, coupled with shorter active fiber lengths is typically employed to maintain high population inversion to aid 976 nm lasing [6]. High CCAR requirement may restrict the cladding size and limit the efficient coupling of pump in step-index LMA fibers [7]. Moreover, the large core in these fibers demands ultra-low numerical aperture (NA) to ensure good beam quality. High CCAR can be achieved in specialty fibers including large-pitch photonic crystal fibers (PCF) and multi-core fibers (MCF), while maintaining large pump waveguide area, but high-gain wavelengths still need to be suppressed to achieve high lasing efficiency at 976 nm. Ref. [8] reported 94 W lasing at 976 nm with 63% efficiency using rod-type PCF but the existence of higher order transverse modes (HOMs) spoiled the beam quality at high power to $M^2 = 2.2$. Moreover, the setup was non-monolithic because of the use of external dielectric mirrors to suppress wavelengths > 1000 nm, making the system prone to misalignments and sensitive to environmental changes.

Distributed filtering of high-gain wavelengths along the active fiber is more advantageous because it allows the use of optimum cavity lengths to fully absorb the pump power and still maintain high population inversion, leading to higher lasing efficiency, while facilitating an all-fiber laser cavity. Ref. [9] reports a photonic bandgap fiber (PBGF) that can inherently suppress four-level wavelengths utilizing bandgap loss. However, the reported fiber had a small mode field area of ~9 μm², rendering it unsuitable for high-power applications. Bend-induced leakage loss is another popular technique to achieve distributed filtering of high-gain ASE and it has been demonstrated in a PBGF to achieve record-high 151 W lasing at 976 nm with 63% efficiency [10] and in an MCF to achieve 25 W lasing at 976 nm with 46% efficiency [11]. Since the wavelength separation between three-level lasing and four-level

lasing is only ~50 nm, bending cannot provide huge differential of loss between the two wavelength bands. For example, in Ref. [10], bend-induced loss at 1030 nm was rather limited to 0.8 dB/m, which necessitated the use of 12 m long fiber length to achieve sufficient filtering of four-level lasing. Bending of lasing fiber may also be associated with mode field distortion and mode shrinking. Besides, the core diameter of fiber employed in this demonstration was ~21 um, suggesting only ~300 um^2 fundamental mode (FM) field area. Moreover, such long cavity lengths are not desirable for high peak power ultrafast lasers at 976 nm [12, 13], which find application in two-photon microscopy [14] and frequency conversion to 488 nm in crystals [13]. To achieve high efficiency ultrafast lasing, it is highly desirable to have an effectively single-moded, large mode area YDF that inherently possesses high differential loss at four-level lasing wavelengths. Though the highest demonstrated power for CW lasing at 976 nm stands at 151 W [10], the highest reported average power for femtosecond pulses at 976 nm is only 4.2 W with 0.5 μJ pulse energy [13]. The setup in [13] utilized a rod type PCF like the one used in Ref. [8] and external dielectric mirrors to suppress four-level lasing wavelengths to generate femtosecond pulses with 14% signal to pump efficiency.

In recent years, research focus on micro-structured fibers has shifted from PCFs to new type of fibers called antiresonant fibers (ARFs) because of their large transmission bandwidths, lower propagation loss, ease of fabrication and efficient suppression of HOMs to achieve effective single-mode propagation [15]. ARFs were initially proposed as hollow-core fibers for laser beam delivery, telecommunication, and nonlinear applications in gas-filled configurations. Recently, all-solid ARF designs have been proposed [16, 17], in which light guidance in silica core, surrounded by high-index antiresonant cladding, follows the same principles as in its hollow-core counterpart. In this letter, we propose an all-solid ytterbium-doped antiresonant fiber (YbARF) design that supports ultra-large mode area (3630 μm^2) for the FM operation and can inherently suppress the otherwise dominant four-level lasing with > 20 dB/m loss for wavelengths > 1010 nm, leading to their efficient suppression even in short fiber lengths (< 1 m). The fiber is designed to have a high HOM suppression ratio throughout the wavelength range of interest, to ensure effective single-mode guidance. Detailed simulations suggest that remarkably high lasing efficiency of up to 85% with respect to launched pump power in single pass configuration can be achieved in the designed fiber. The design principles can be universally applied to enhance lasing at low-gain wavelengths in neodymium-doped, thulium-doped, and erbium-doped fiber lasers and amplifiers by suppression of high-gain ASE.

1. Proposed fiber design

Light guidance through low-index core in an ARF can be explained by inhibited coupling of FM with lossy cladding modes by virtue of transverse phase mismatch and low spatial overlap among them [18]. Resonant coupling of FM to cladding modes is, however, possible near the cutoff wavelengths (λ_R) of the latter, which are determined by the wall thickness t of cladding capillaries, and given by $\lambda_R = (2t/m)\sqrt{(n_1^2 - n_2^2)}$, where n_1 is the refractive index of background material, n_2 is the refractive index of cladding capillaries and m is an integer, also referred to as order of resonance. A transmission spectrum of these fibers is, therefore, characterized by wide transmission bands interspersed with resonant wavelength bands, in which light is not confined to the core and leaks out to the lossy cladding region. The resonant bands are therefore characterized by orders of magnitude higher confinement loss (CL) as compared to the antiresonant band. The high CL region in an ARF is, however, not just restricted to single resonant wavelengths, but extends to much shorter wavelengths due to finite capillary wall thickness [18]. This is because as the capillary thickness increases, the cutoff wavelengths of the capillary glass modes spread wider. Coupling to these modes is characterized by distinct high loss peaks on the short wavelength edge in each resonance band (m=1, 2 etc.), and hence broadening the resonance band.

To achieve high-efficiency lasing at 976 nm, we have designed a single-layer, six-tube lattice YbARF with background material as silica glass (n_1=1.45). The core (shaded circle in Fig. 1a)) is assumed to be alumino-phospho-silicate glass with Yb doping, which is known to exhibit efficient, photodarkening-free lasing at 976 nm [19]. The core is co-doped with fluoride ions to match the index with background glass, like the case of all-solid PBGFs [19]. The cladding capillaries are assumed to be germanium-doped with refractive index n_2 =1.48 (Please refer to Fig. 1 a). The ytterbium ion concentration is chosen to be 4×10^{25} m^{-3}, which is standard value for conventional Yd-doped fibers. The core diameter D is chosen to be 90 μm and inner diameter d of cladding capillaries is optimized to be 0.67 times D. Optimization of the ratio of inner diameter of cladding capillaries to the core diameter ensures that the first HOM is phase-matched to a lossy cladding mode and suffers high propagation loss throughout the wavelength range in consideration. The upper limit on size of the core is governed by the ability of six-capillary structure to provide effectively single mode operation along with low loss for FM [16].

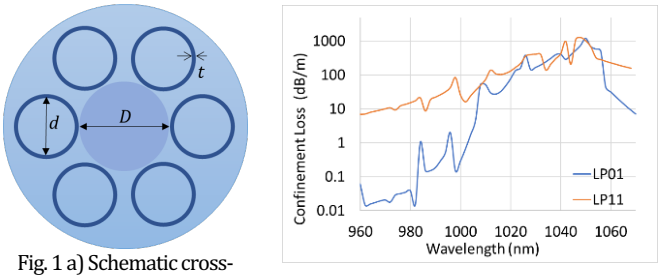

Fig. 1 a) Schematic cross-section of proposed YbARF b) Spectral variation of confinement loss for the two lowest order modes in designed YbARF

The capillary wall thickness is optimized to be 1.77 μm, so that the first order resonant wavelength (λ_R) falls at 1050 nm . The short wavelength edge of the resonant band extends up to 1000 nm and the high-loss region covers the entire wavelength region corresponding to four-level lasing in ytterbium. Modal characteristics of the YbARF are simulated by applying full vector finite element method using COMSOL Multiphysics. Perfectly matched layers (PMLs) with their standard cylindrical definition have been used to surround the calculation domain. Extremely fine maximum mesh size was chosen, and convergence studies were carried out over mesh parameters and PML thickness to ensure numerical stability. The effect of material dispersion was also included in simulations. Fig. 1 b) shows the spectral variation of CL for the FM and the 1st HOM in the YbARF. At 976 nm, the FM is characterized by CL of 0.03 dB/m, while the 1st HOM would suffer a propagation loss of 12 dB/m, which is three orders of magnitude

higher than the propagation loss of FM. Unlike in PBGF, the resonant out-coupling of HOMs is not restricted to a narrow wavelength range in an ARF, and the 1st HOM in the Yb-ARF suffers > 10 dB/m loss over the entire spectrum covering emission by Yb-ions, which is an important criterion to ensure single transverse mode lasing [21]. Fig. 2a and 2b show the mode field profiles of the FM and 1st HOM at 976 nm and 1030 nm, respectively. The FM has a mode field diameter of 68 μm (3630 μm² mode area) at 976 nm.

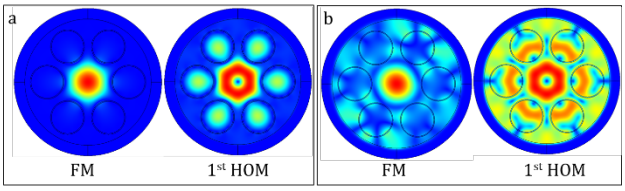

Fig. 2 Mode profiles of FM and 1st HOM at a) 976 nm and b) 1030 nm

2. High efficiency 976 nm lasing in YbARF

The YbARF can be effectively pumped using standard high-power diode lasers at 915 nm with delivery fibers having NA = 0.22 and core/cladding ratio of 105/125 um. Even though 915 nm lies in the antiresonant wavelength band of the YbARF, the high NA pump beam will not just be confined to the core (NA ~ 0.03), but would propagate freely across the fiber cross-section, leading to its efficient absorption by the doped core. The YbARF is proposed to be jacketed with a low-index fluorine-doped silica tube that would guide the pump beam by virtue of total internal reflection with 0.22 NA. The pump waveguide diameter is chosen to be 200 μm, like in rod-type PBGFs with similar core diameter [8]. The overall diameter after the jacketing tube can be much thicker to avoid any possible micro-bending related issues.

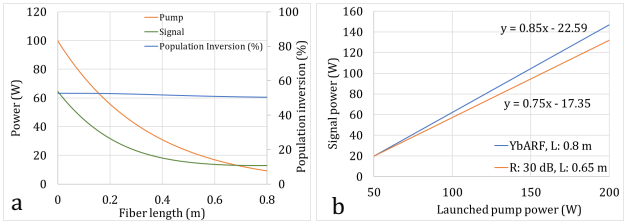

Fig. 3 a) Variation of pump power, signal power and population inversion along fiber length in the YbARF cavity b) Signal versus launched pump power in the YbARF cavity (blue) and in a similar cavity with dichroic mirror having 30 dB lower reflectivity instead of high propagation loss for wavelengths > 1000 nm (orange); fiber lengths are optimized for maximum lasing power in each cavity

We studied the performance of a free-running laser cavity set by Fresnel reflection (~4%) at pump output end and high reflection (99%) at the other, in single-pass configuration for pump, using a commercial software Fiber Power by RP Photonics. Fig. 3a shows the evolution of pump power, signal power and population inversion along the fiber length for a launched pump power of 100 W. The fiber length (L) is optimized at 0.8 m, to achieve maximum lasing power output at 976 nm. We note that in the presence of strong distributed filtering of high-gain wavelengths, >90% pump could be absorbed in the fiber while still maintaining population inversion > 50% to support 976 nm lasing. Fig. 3b shows the simulated variation of lasing power versus launched pump power promising a high slope efficiency of 85% in the designed YbARF cavity. The predicted results supersede all previous state-of-the-art demonstrations for 976 nm lasing [8-10], because of its strong suppression of four-level lasing in a distributed manner coupled with high CCAR.

We put forth evidence of the effectiveness of the distributed filtering effect. Even though previously demonstrated PCF based rod-type fiber [8] have similar CCAR to the proposed YbARF, the lasing efficiency was lower in single-pass pump configuration because of the use of external dielectric mirrors to suppress four-level lasing. Apart from the fact that external reflectivity mirrors lead to additional coupling losses, our simulations reveal that standard reflectivity filters offering suppression of reflection by 30 dB are not sufficient to suppress four-level lasing enough for one to operate at fiber length optimized for maximum three-level lasing efficiency. As a result, one is bound to use shorter fiber length to maintain population inversion > 50% to support 976 nm lasing, which in turn leaves a larger fraction of unused pump power, necessitating the use of double-pass configuration to enhance efficiency [8].

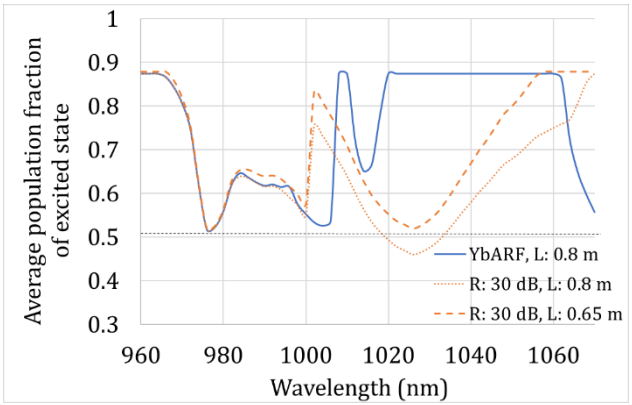

Fig. 4 Spectral variation of average population fraction of excited state along fiber length in YbARF and in a similar YDF cavity without distributed spectral loss but with discrete reflectivity filter having reflectivity R lower by 30 dB for wavelengths > 1000 nm

To study this effect, we simulated lasing in a YDF cavity identical (in terms of fiber and cavity parameters) as the designed YbARF cavity, except for no additional propagation loss at high-gain wavelengths and with an external dielectric mirror (like the one used in Ref. [8]) having 85% coupling and reflectivity (R) 30 dB lower for wavelengths > 1000 nm. Fig. 4 shows the simulated variation of fraction of average population inversion (N_{2av}) over the fiber length for different cavity configurations. The wavelength corresponding to lowest value of N_{2av} is expected to be the lasing wavelength for that cavity [22]. We note that discrete suppression of four-level lasing by 30 dB, in a 0.8 m long cavity with > 90% pump absorption, is not sufficient to achieve three-level lasing at 976 nm (dotted orange curve) and the lasing wavelength lies at around 1028 nm. One, therefore, needs to operate with shorter fiber length (L:0.65 m, optimized for maximum output power) to sustain high enough population inversion along the fiber length to achieve lasing at 976 nm (orange dashed curve). As a result, such a cavity has larger fraction of residual pump and is therefore characterized by

lower lasing efficiency of 75% (orange curve in Fig. 3b). We can thus conclude that strong distributed filtering of high-gain wavelengths results in high lasing efficiency at 976 nm.

3. Fabrication and Tolerance

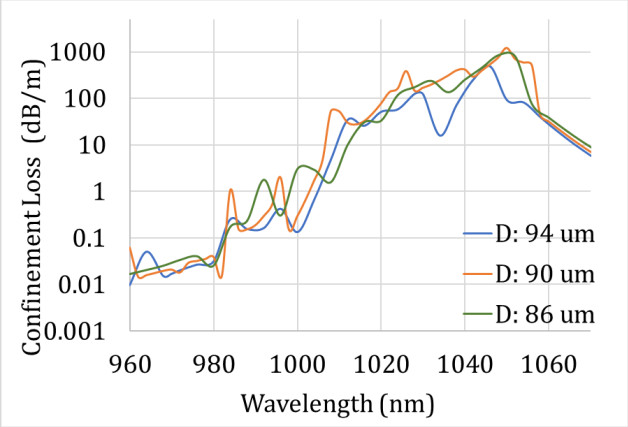

Fig. 5 Spectral variation of *CL* for FM in YbARF for different core diameters, keeping *d/D* and *t* constant

Fabrication of doped solid fibers is a mature technology and one possible scheme for fabrication of an all solid antiresonant fiber is discussed in Ref. [23]. It employs insertion of doped capillaries fabricated using outside vapor deposition technique into doped-core preform using ultrasonic drilling. Alternatively, the standard stack-and-draw technique can be easily adopted for this kind of fibre fabrication. The YbARF is susceptible to bending losses by virtue of its ultra large mode area and low NA, so we propose it to be surrounded by a thick jacket, analogous to the one used in rod-type PBGFs, to keep it straight. The only crucial fiber parameter in the fabrication of YbARF is the capillary wall thickness, as it decides the spectral variation of fundamental mode loss. Simulations reveal that the tolerance on capillary wall thickness is within 1% to achieve > 20 dB difference between propagation loss of 976 nm and high-gain wavelengths corresponding to four-level lasing. The spectral variation of loss is, however, more tolerant to the variation in core diameter. Therefore, capillary wall thickness t can be precisely controlled by scaling the preform to fiber ratio during fiber drawing. Fig. 5 shows the spectral variation of *CL* for FM for different core diameters D, keeping the d/D ratio and t constant. Since the suppression of the 1st HOM is governed only by the d/D ratio, the overall scaling of fiber dimensions does not adversely affect the single-mode operation of Yb-ARF.

4. Conclusions

We proposed and analyzed a novel all-solid antiresonant fiber design for single-mode, ultra-large mode area three-level lasing in ytterbium ions. The design is optimized such that the wavelengths corresponding to four-level lasing lie in the resonance band and suffer high confinement loss. We show that strong distributed filtering of high-gain wavelengths enables maintenance of high population inversion along the fiber and promise high efficiency (85%) three-level lasing at 976 nm in a short length (0.8 m) of YbARF. The designed YbARF is characterized by ultra-large fundamental mode area ~3630 μm² and > 10 dB/m suppression of HOMs to facilitate near-diffraction limited lasing. The design principles can be extended to shift the wavelength band of operation in other rare-earth doped (thulium, erbium, neodymium) fiber lasers and amplifiers.

Funding. National Research Foundation Singapore, Quantum Engineering Programme.

Acknowledgments. C. Goel thanks Dr. Huizi Li, Nanyang Technological University, for providing spectroscopic data for ytterbium ions in alumino-phospho-silicate glass.

Disclosures. The authors declare no conflicts of interest.

References

1. L. Dong, X. Peng, and J. Li, J. Opt. Soc. Am. B 24, 1689-1697 (2007)
2. J. Limpert, F. Stutzki, F. Jansen, H-J Otto, T. Eidam, C. Jauregui and A. Tu¨nnermann, Light Sci Appl 1, e8 (2012)
3. J. Ji, S. Raghuraman, X. Huang, J. Zang, D. Ho, Y. Zhou, Y. Benudiz, U. Ben Ami, A. A. Ishaaya, and S. Yoo, Opt. Lett. 43, 3369-3372 (2018)
4. X. Ma, C. Zhu, I-N Hu, A. Kaplan, and A. Galvanauskas, Opt. Express 22, 9206-9219 (2014)
5. Pingxue Li, Shuzhen Zou, Xuexia Zhang, Zhenao Bai, Gang Li, A 980nm Yb-doped single-mode fiber laser pumped by a 946nm Q-switched Nd:YAG laser, Optics & Laser Technology, 42, 1229-1232 (2010)
6. S. S. Aleshkina, M. E. Likhachev, D. S. Lipatov, O. I. Medvedkov, K. K. Bobkov, M. M. Bubnov, and A. N. Guryanov, Fiber Lasers XIII Technol. Syst. Appl. 9728(October 2017), 97281C (2016).
7. S. S. Aleshkina, A. E. Levchenko, O. I. Medvedkov, K. K. Bobkov, M. M. Bubnov, D. S. Lipatov, A. N. Guryanov, and M. E. Likhachev, IEEE Photonics Technol. Lett. 30(1), 127–130 (2018).
8. F. Röser, C. Jauregui, J. Limpert, and A. Tünnermann, Opt. Express 16, 17310-17318 (2008)
9. V. Pureur, L. Bigot, G. Bouwmans, Y. Quiquempois, M. Douay, and Y. Jaouen, Appl. Phys. Lett. 92(6), 061113 (2008).
10. W. Li, T. Matniyaz, S. Gafsi, M. T. Kalichevsky-Dong, T. W. Hawkins, J. Parsons, G. Gu, and L. Dong, Opt. Express 27, 24972-24977 (2019)
11. H. Li, J. Zang, S. Raghuraman, S. Chen, C. Goel, N. Xia, A. Ishaaya, and S. Yoo, Opt. Express 29, 21992-22000 (2021)
12. S. S. Aleshkina, D. S. Lipatov, V. V. Velmiskin, V. Temyanko and M. E. Likhachev, IEEE Photonics Technol. Lett., 32, 13, 811-814, (2020)
13. J. Lhermite, G. Machinet, C. Lecaplain, J. Boullet, N. Traynor, A. Hideur, and E. Cormier, Opt. Lett. 35, 3459-3461 (2010)
14. R.D. Niederriter, B.N. Ozbay, G.L. Futia, E.A. Gibson, J. T. Gopinath, Biomed. Opt. Express 8,1 315-322, (2016)
15. W. Ding, Y. Wang, S. Gao, M. Wang and P. Wang, IEEE J. Sel. Top. Quantum Electron., 26 (4), 1-12, (2020)
16. X. Zhang, S. Gao, Y. Wang, W. Ding, and P. Wang, High Power Laser Sci. Eng. 9: e23 (2021)
17. X. Zhen, X. Wang, S. Lou, Z. Tang, H. Jia, S. Gu and J. Han, Opt. Lett. 46, 1908-1911 (2021)
18. L. Vincetti and V. Setti, Opt. Express 18, 23133–23146 (2010).
19. H. Li, S. Chen, R. Sidharthan, J. Ma, N. Xia, C.J. Chang, J. Kim and S. Yoo, IEEE Photonics Technol. Lett., 32 (23), pp. 1457-1460, 2020
20. J. Limpert, O. Schmidt, J. Rothhardt, F. Röser, T. Schreiber, A. Tünnermann, S. Ermeneux, P. Yvernault, and F. Salin, Opt. Express 14, 2715 (2006).
21. A. Steinkopff, C. Jauregui, F. Stutzki, J. Nold, C. Hupel, N. Haarlammert, J. Bierlich, A. Tünnermann, and J. Limpert, Opt. Lett. 44, 650-653 (2019)
22. R. Paschotta, Encyclopedia of Laser Physics and Technology (Wiley-VCH, 2008) https://www.rp-photonics.com/software_news_2017_03_28.html
23. Z. Xing, X. Wang, S. Gu, S. Lou, Results in Physics, 29, 104700, (2021)